Cumhuriyet Sci. J., 46(2) (2025) 338-347
DOI: https://doi.org/10.17776/csj.1665644

Cumhuriyet Science Journal

| csj.cumhuriyet.edu.tr | Founded: 2002 ISSN: 2587-2680 e-ISSN: 2587-246X Publisher: Sivas Cumhuriyet University

Investigation of the Activity of Benzenesulfonamide Derivative Molecules Against Gastric Cancer Proteins with Gaussian Calculations and Docking Analysis

Burak Tüzün[1,a,*]

[1] *Plant and Animal Production Department, Technical Sciences Vocational School of Sivas, Sivas Cumhuriyet University, Sivas, Türkiye*

**Corresponding author*

Research Article

History
Received: 26/03/2025
Accepted: 21/05/2025

ABSTRACT

While gastric cancer poses a significant problem in terms of global health with its high mortality rates, the limitations in current treatment methods necessitate the identification of new molecular targets and potential drug candidates. Benzenesulfonamide derivatives are among the compounds that have attracted attention in recent years due to their structural diversity and biological activity potential. In the study, the electronic properties, orbital distributions and thermodynamic stabilities of benzenesulfonamide derivative molecules were calculated using the Gaussian program; thus, the reactivity tendencies of the molecules and their interaction potential with target proteins were tried to be revealed. The calculations were made in the 6-31++g(d,p) basis set at the B3LYP, HF, M062X level. The theoretical data obtained were supported by molecular docking analyses; Docking studies have evaluated the binding affinities and interaction sites of benzenesulfonamide derivatives with the identified gastric cancer proteins, which are PDB ID: 3MAX and 4BKX proteins, in detail. Then, MM-GBSA values were calculated for the molecule with the highest activity among these molecules. Finally, ADME/T calculations were performed to examine the drug potential of the molecules.

Keywords: Benzenesulfonamide, DFT, Molecular docking, MM-GBSA, ADME/T.

[a] *theburaktuzun@yahoo.com* *https://orcid.org/0000-0002-0420-2043*

Introduction

Gastric cancer is a serious health problem with high incidence rates worldwide, especially in regions such as Asia and Eastern Europe. This malignancy occurs as a result of uncontrolled growth of cells in the gastric mucosa and is usually triggered by a combination of Helicobacter pylori infection, genetic predisposition, irregular diet, high salt consumption, smoking and environmental factors. The absence of obvious symptoms in the early stage leads to late diagnosis and the detection of the disease in advanced stages, which negatively affects treatment options and prognosis. Although traditional treatment methods include surgical intervention, chemotherapy, radiotherapy and targeted therapies, multidisciplinary approaches are increasingly gaining importance in order to determine the most appropriate strategy for each patient [1].

Theoretical calculations play an important role in understanding the molecular complexity of gastric cancer and developing new disease-specific treatment strategies. In this context, quantum chemical calculations using the Gaussian program provide detailed analysis of the electron distribution, reactivity parameters and thermodynamic properties of target molecules [2]. Gaussian helps to deeply understand the molecular structure of proteins and other biological targets that affect gastric cancer with basic calculations such as the calculation of molecular orbitals, ionization potentials and electron affinities.

At the same time, the Maestro (Schrödinger) platform offers the opportunity to visualize in detail the interactions of potential drug candidates with target proteins through molecular modeling, docking studies and dynamic simulations. This program provides powerful tools to predict how drugs interact with active sites, their binding affinities and interaction mechanisms by integrating with structural biology data [3]. These approaches, supported by theoretical calculations, when combined with experimental data, allow for a better understanding of the molecular pathogenesis of gastric cancer and the development of personalized treatment strategies.

In conclusion, in the development of treatment and diagnostic methods for gastric cancer, the use of advanced theoretical computational tools such as Gaussian and Maestro Schrödinger, as well as experimental data obtained from clinical applications, plays a critical role in revealing the molecular basis of the disease. This integrated approach allows the development of promising, comprehensive and innovative strategies in terms of early diagnosis, increasing the effectiveness of treatment and identifying new drug candidates.

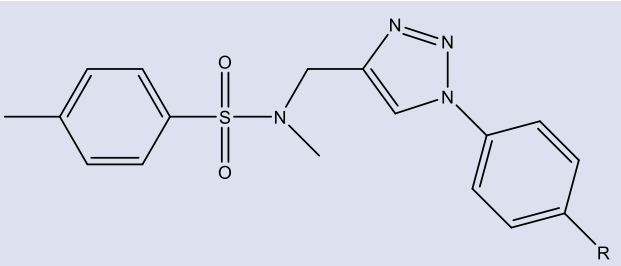

Scheme 1. Main skeleton of benzenesulfonamide derivative molecules

In this study, molecule 1 (N-((1-(4-methoxyphenyl)-1H-1,2,3-triazol-4-yl)methyl)-N,4-dimethylbenzenesulfonamide), molecule 2 (N,4-dimethyl-N-((1-(p-tolyl)-1H-1,2,3-triazol-4-yl)methyl)benzenesulfonamide), molecule 3 (N-((1-(4-isopropylphenyl)-1H-1,2,3-triazol-4-yl)methyl)-N,4-dimethylbenzenesulfonamide), molecule 4 (N-((1-(4-chlorophenyl)-1H-1,2,3-triazol-4-yl)methyl)-N,4-dimethylbenzenesulfonamide), molecule 5 (N-((1-(4-fluorophenyl)-1H-1,2,3-triazol-4-yl)methyl)-N,4-dimethylbenzenesulfonamide), molecule 6 (N,4-dimethyl-N-((1-(4-nitrophenyl)-1H-1,2,3-triazol-4-yl)methyl)benzenesulfonamide), molecule 7 (Ethyl-4-(((N,4-dimethylbenzenesulfonamido)methyl)-1H 1,2,3-triazol-1-yl)benzoate), and molecule 8 (N-((1-(4-acetylphenyl)-1H-1,2,3-triazol-4-yl)methyl)-N,4-dimethylbenzenesulfonamide) molecules were all synthesized by Şahin and co-worker [4] in Figure 1. Then, the quantum chemical parameters of these molecules were calculated with the Gaussian package program. Calculations using the 6-31++g(d,p) basis set in the B3LYP, HF, and M06-2x [5–7] techniques were performed using these programs. Then, the activities of the molecules against various proteins, which are PDB ID: 3MAX and 4BKX proteins [8,9], were compared. The interaction values of the molecule with the highest activity were examined by MM-GBSA calculation. Finally, the drug properties of the molecules were examined by ADME/T analysis of the molecules.

Theoretical Methods

The chemical and biological characteristics of molecules may be greatly inferred from theoretical calculations. Theoretical simulations provide a great deal of information about quantum chemical parameters. The computed parameters are used to explain the chemical activity of the molecules. Molecules are calculated using a variety of applications. Gaussian09 RevD.01 and GaussView 6.0 are the names of these different applications [10,11]. Calculations using the 6-31++g(d,p) basis set in the B3LYP, HF, and M06-2x [5-7] techniques were performed using these programs. Several quantum chemical parameters have been discovered as a result of these quantum chemistry computations. The following displays the computed parameters, each of which denotes a distinct molecular chemical property [12,13]. The formulas for calculating these parameters are given in equations 1-3.

$$\chi = -\left(\frac{\partial E}{\partial N}\right)_{v(r)} = \frac{1}{2}(I + A) \cong \frac{1}{2}(E_{HOMO} + E_{LUMO}) \quad (1)$$

$$\eta = -\left(\frac{\partial^2 E}{\partial N^2}\right)_{v(r)} = \frac{1}{2}(I - A) \cong -\frac{1}{2}(E_{HOMO} - E_{LUMO}) \quad (2)$$

$$\sigma = 1/\eta \qquad \omega = \chi^2/2\eta \qquad \varepsilon = 1/\omega \quad (3)$$

The biological activities of molecules are compared to biological materials using molecular docking calculations. Molecular docking calculations were performed using Schrödinger's Maestro Molecular modeling platform (version 13.4) [14]. There are several stages involved in calculations. Every stage is carried out in a unique way. Proteins were prepared in the first phase using the protein preparation module [15]. The proteins' active sites were identified in this module. The next stage involves preparing the compounds under study. The LigPrep module [16] is ready for computations utilizing optimized structures once the molecules have first been optimized in the Gaussian software application. Following preparation, the interactions between the compounds and the cancer protein were investigated using the Glide ligand docking module [17,18]. All computations were performed using the OPLS4 technique. Finally, the pharmacological potential of the investigated compounds will be investigated using ADME/T analysis (absorption, distribution, metabolism, excretion, and toxicity). The effects and reactions of chemicals in human metabolism were predicted using the Schrödinger software's Qik-prop module [19].

Result and Discussion

Knowledge of terms like the ΔE energy gap, E_{HOMO}, E_{LUMO}, chemical hardness, softness, electronegativity, and chemical potential is necessary to comprehend the electronic structure and chemical characteristics of molecules [20]. These are the fundamental standards used to evaluate the stability and reactivity of a chemical.

The difference in energy levels between a molecule's highest occupied molecular orbital (HOMO) and lowest unoccupied molecular orbital (LUMO) is measured by the energy gap, or ΔE [21]. To fully comprehend the electrical stability and reactivity of a molecule, one must have a thorough comprehension of this value. While a larger ΔE value suggests a more stable molecular structure, a smaller ΔE value indicates stronger molecular reactivity [22].

In the context of molecular orbital energy, E_{HOMO} and E_{LUMO} stand for the energy of the highest occupied molecular orbital and the lowest unoccupied molecular orbital, respectively. While the LUMO determines a molecule's ability to take electrons, showing electrophilic behavior, the HOMO controls a molecule's tendency to give electrons, indicating nucleophilic activity [21]. To comprehend the mechanics of electron transport in chemical processes, one must have a thorough knowledge of the energy difference between the HOMO and LUMO states.

The ability of a molecule to withstand changes brought on by outside influences is known as chemical hardness.

Harder molecules are less reactive and have improved structural stability. Chemical softness is a measure of a molecule's reactivity; molecules that are softer are more vulnerable to changes in their chemical structure. The ideas of softness and hardness may help forecast the formation of chemical bonds and clarify the acid-base characteristics of molecules [23].

One important factor that determines the polarity of chemical bonds is electronegativity. It is a term used to describe the propensity of an atom or molecule to draw bonding electrons. Compounds with higher electronegativity are better at drawing electrons and displaying electrophilic properties during chemical reactions.

Chemical potential, as described in, quantifies the energy change inside a molecule and shows how the system reacts to variations in electron density [24]. This figure is an important indication in the measurement of molecule stability and reaction energy.

When combined, these ideas provide a thorough foundation for comprehending molecules' electrical structure, stability, and chemical reactivity. When combined with ΔE, the evaluation of HOMO and LUMO energy levels provides a useful way to predict chemical reactivity. Characteristics like electronegativity, softness, and chemical hardness are essential for understanding how molecules react to outside stimuli. All of the factors are listed in detail in Table 1. and Figure 1..

Table 1. The calculated quantum chemical parameters of molecules.

	E_{HOMO}	E_{LUMO}	I	A	ΔE	η	μ	χ	PA	ω	ε	dipol	Energy
B3LYP/6-31g LEVEL													
1	-6.2249	-1.3617	6.2249	1.3617	4.8633	2.4316	0.4112	3.7933	-3.7933	2.9587	0.3380	4.2117	-40849.7670
2	-6.3509	-1.4283	6.3509	1.4283	4.9226	2.4613	0.4063	3.8896	-3.8896	3.0734	0.3254	4.6627	-38803.3891
3	-6.3479	-1.4169	6.3479	1.4169	4.9310	2.4655	0.4056	3.8824	-3.8824	3.0568	0.3271	4.6850	-40941.6618
4	-6.5117	-1.7454	6.5117	1.7454	4.7664	2.3832	0.4196	4.1285	-4.1285	3.5761	0.2796	3.6492	-50240.6179
5	-6.4970	-1.5867	6.4970	1.5867	4.9103	2.4552	0.4073	4.0419	-4.0419	3.3270	0.3006	3.6481	-40434.7499
6	-6.7898	-3.2042	6.7898	3.2042	3.5857	1.7928	0.5578	4.9970	-4.9970	6.9638	0.1436	5.3898	-43299.0681
7	-6.5237	-2.1704	6.5237	2.1704	4.3533	2.1767	0.4594	4.3471	-4.3471	4.3408	0.2304	5.2673	-45003.6194
8	-6.5683	-2.3987	6.5683	2.3987	4.1696	2.0848	0.4797	4.4835	-4.4835	4.8210	0.2074	5.7166	-41887.1637
HF/6-31g LEVEL													
1	-8.9738	0.9568	8.9738	-0.9568	9.9306	4.9653	0.2014	4.0085	-4.0085	1.6181	0.6180	4.7966	-40647.3515
2	-8.9175	0.9608	8.9175	-0.9608	9.8784	4.9392	0.2025	3.9783	-3.9783	1.6022	0.6241	4.6128	-38610.8882
3	-8.9017	0.9391	8.9017	-0.9391	9.8408	4.9204	0.2032	3.9813	-3.9813	1.6107	0.6208	4.6529	-40733.8299
4	-9.1496	0.9426	9.1496	-0.9426	10.0922	5.0461	0.1982	4.1035	-4.1035	1.6685	0.5993	3.2312	-50036.8689
5	-9.1883	0.9407	9.1883	-0.9407	10.1290	5.0645	0.1975	4.1238	-4.1238	1.6789	0.5956	3.2566	-40239.4319
6	-9.4786	0.6803	9.4786	-0.6803	10.1589	5.0795	0.1969	4.3992	-4.3992	1.9050	0.5249	4.8067	-43086.1026
7	-9.1992	0.9568	9.1992	-0.9568	10.1559	5.0780	0.1969	4.1212	-4.1212	1.6724	0.5980	5.4619	-44777.4174
8	-9.2182	0.8811	9.2182	-0.8811	10.0993	5.0497	0.1980	4.1685	-4.1685	1.7206	0.5812	5.8118	-41678.4222
M062X/6-31g LEVEL													
1	-7.4024	-0.5448	7.4024	0.5448	6.8576	3.4288	0.2916	3.9736	-3.9736	2.3025	0.4343	4.7982	-40836.0737
2	-7.5618	-0.5606	7.5618	0.5606	7.0013	3.5006	0.2857	4.0612	-4.0612	2.3558	0.4245	4.7342	-38790.3383
3	-7.7221	-0.4816	7.7221	0.4816	7.2405	3.6202	0.2762	4.1019	-4.1019	2.3238	0.4303	5.1803	-40927.5710
4	-7.7382	-0.6566	7.7382	0.6566	7.0815	3.5408	0.2824	4.1974	-4.1974	2.4879	0.4019	5.7329	-50227.5167
5	-7.7270	-0.6093	7.7270	0.6093	7.1177	3.5589	0.2810	4.1681	-4.1681	2.4409	0.4097	5.5987	-40421.5428
6	-8.0274	-1.9552	8.0274	1.9552	6.0723	3.0361	0.3294	4.9913	-4.9913	4.1027	0.2437	8.5469	-43284.5808
7	-7.7624	-1.0621	7.7624	1.0621	6.7003	3.3502	0.2985	4.4122	-4.4122	2.9055	0.3442	4.9684	-44988.2096
8	-7.7967	-1.2640	7.7967	1.2640	6.5327	3.2663	0.3062	4.5303	-4.5303	3.1417	0.3183	5.9869	-41873.0026

Koopman's theorem [25,26], a fundamental concept in molecular orbital theory, connects a molecule's electron affinity and ionization energy to its HOMO and LUMO energy levels. The theory states that the energy of the HOMO is equivalent to the ionization energy of the molecule, whereas the energy of the LUMO indicates the electron affinity of the molecule. This method offers a strong tool for predicting the electrical properties and reactivity of molecules. The findings are only guesses that could need more complex calculations to support, despite the fact that the theory does not take electron-electron interactions into account.

The Hard and Soft Acid-Base (HSAB) paradigm [27] was created to understand acid-base chemistry. According to this view, hard acids interact strongly with hard bases, while soft acids create strong surfaces with soft bases [28]. According to this theory, a system will often adopt a structure with increasing hardness since it is more stable and less reactive. This concept offers a helpful foundation for predicting the stability of molecules and chemical processes. The idea of maximum hardness is often used, particularly in the assessment of transition states and the creation of reactive intermediates.

These three core ideas provide a theoretical and practical basis for a comprehensive understanding of the characteristics of molecular bonding and reactivity. The HSAB principle explains the nature of acid-base interfaces [29], Koopman's theorem analyzes electron transport channels, and PMH largely predicts molecular stability [30]. Combining these methods might result in a thorough understanding of the behavior of chemical systems.

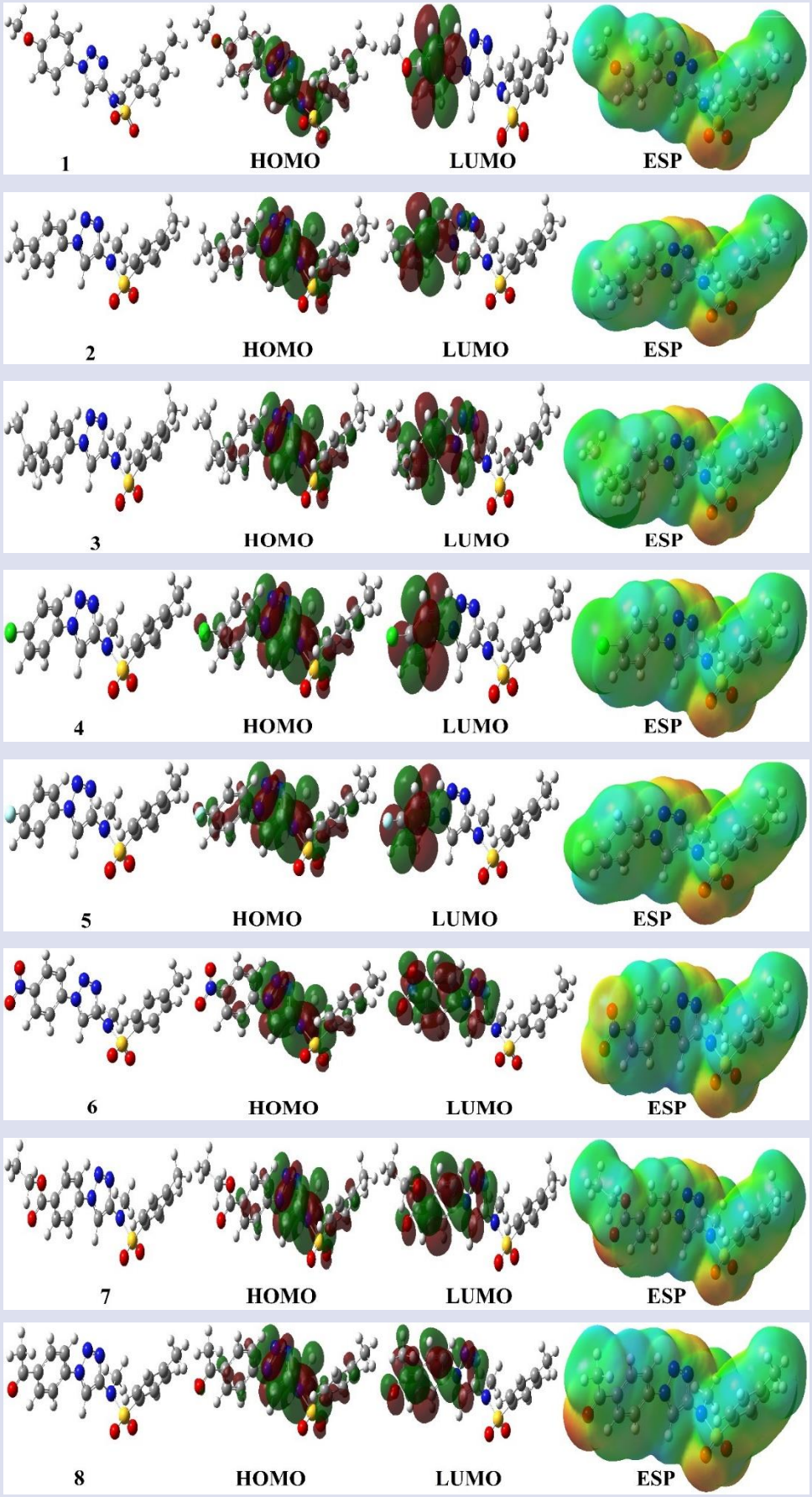

Figure 2. Representations of optimize structure, HOMO, LUMO, and ESP of molecules

As a result of the gaussian calculations, many quantum chemical parameters have been calculated. In these calculations, one of the first important parameters is the HOMO energy value of the molecules, and when the

comparison is made according to the numerical values of these parameters, it is seen that molecule 1 has the highest activity at all three levels. On the other hand, when the comparison is made according to the numerical value of the LUMO parameter of the molecules, it is seen that molecule 6 has the highest activity at the B3LYP and M062X levels and molecule 8 has the highest activity at the HF level. When the comparison is made according to the energy gap values of the molecules, it is seen that molecule 6 has the highest activity at the B3LYP and M062X levels and molecule 3 has the highest activity at the HF level. Finally, when the energy value of the electronegativity parameter of the molecules is examined, it is seen that molecule 1 has the highest activity at both the B3LYP and M062X levels and molecule 2 has the highest activity at the HF level.

Table 2. Numerical values of the docking parameters of molecule against enzymes

4BKX	Docking Score	Glide ligand efficiency	Glide hbond	Glide evdw	Glide ecoul	Glide emodel	Glide energy	Glide einternal	Glide posenum
1	-3.04	-0.12	0.00	-27.00	-3.74	-34.75	-30.74	4.50	234
2	-2.84	-0.12	0.00	-25.34	-3.45	-32.38	-28.79	3.60	352
3	-3.29	-0.13	0.00	-32.05	-2.92	-39.39	-34.97	3.14	126
4	-3.36	-0.14	0.00	-29.81	-0.34	-36.36	-30.15	0.34	378
5	-3.50	-0.15	0.00	-29.22	-0.38	-36.57	-29.60	0.69	244
6	-2.60	-0.10	0.00	-32.24	-2.06	-36.42	-34.30	3.94	238
7	-3.07	-0.11	0.00	-33.34	-2.54	-39.62	-35.87	6.20	322
8	-3.54	-0.14	0.00	-29.26	-3.06	-38.37	-32.32	4.06	278
3MAX	**Docking Score**	**Glide ligand efficiency**	**Glide hbond**	**Glide evdw**	**Glide ecoul**	**Glide emodel**	**Glide energy**	**Glide einternal**	**Glide posenum**
1	-1.76	-0.07	0.00	-20.44	-5.31	-24.26	-25.76	2.66	322
2	-2.41	-0.10	0.00	-27.33	-0.47	-29.53	-27.80	4.09	95
3	-3.03	-0.12	0.00	-29.99	-2.70	-36.56	-32.69	5.13	254
4	-3.55	-0.15	0.00	-27.60	-7.47	-40.74	-35.08	2.75	129
5	-3.44	-0.14	0.00	-26.31	-7.45	-38.98	-33.76	2.71	243
6	-1.66	-0.06	0.00	-26.75	-2.16	-26.50	-28.91	3.19	274
7	-3.42	-0.12	0.00	-33.15	-7.94	-47.46	-41.08	3.85	294
8	-3.22	-0.12	0.00	-31.44	-3.67	-40.80	-35.11	3.66	104

Recent studies indicate that the comparison of molecules' biological activities has been significantly expedited and made simpler by the extensive use of theoretical research and technological breakthroughs [31]. This is the outcome of widespread use of these two research methodologies. This assertion is supported by the findings of current research. Calculations have significantly sped up and simplified the process of identifying the most effective and successful medications before experimental testing [32]. The theoretical computations revealed a number of factors. This method is utilized to ascertain the relationship between the numerical values of these parameters and the biological activities of molecules. This is done in order to assess the biological parameters. The interactions between various proteins and chemicals are the most significant factor influencing the activities outlined [33]. The widespread nature of these interactions ultimately inhibits the proteins. This is the mechanism via which inhibition occurs. The way chemicals interact with proteins determines their energy levels. Molecules and proteins interact by π-π interactions, halogen interactions, hydrogen bonds, and polar and hydrophobic contacts [31–33]. Molecular interaction is necessary for equilibrium to stay constant. Comprehensive studies of these chemical interactions have shown that there are many different ways in which chemicals and proteins interact. All of the characteristics are in Table 2, and all of the figures are in Figures 2-3.

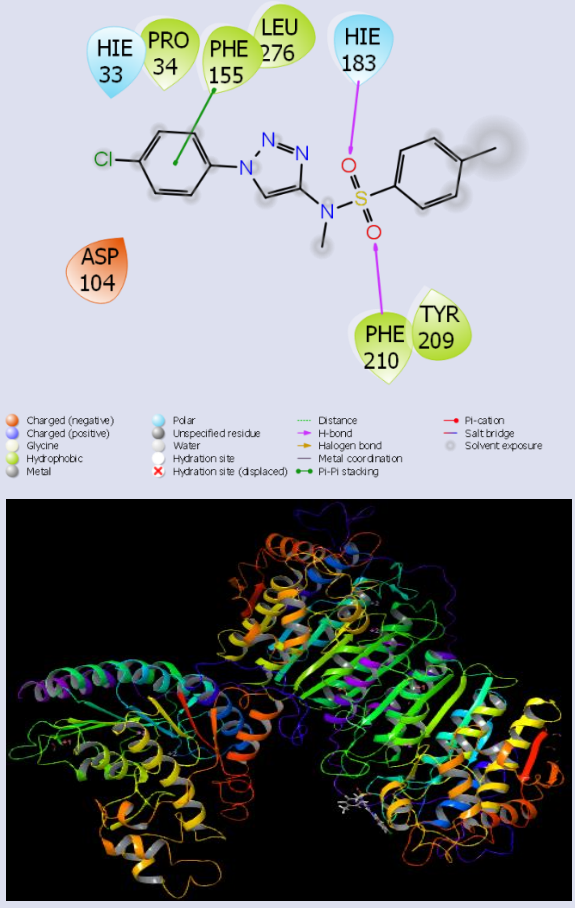

Figure 2. Presentation interactions of molecule 4 with 3MAX protein

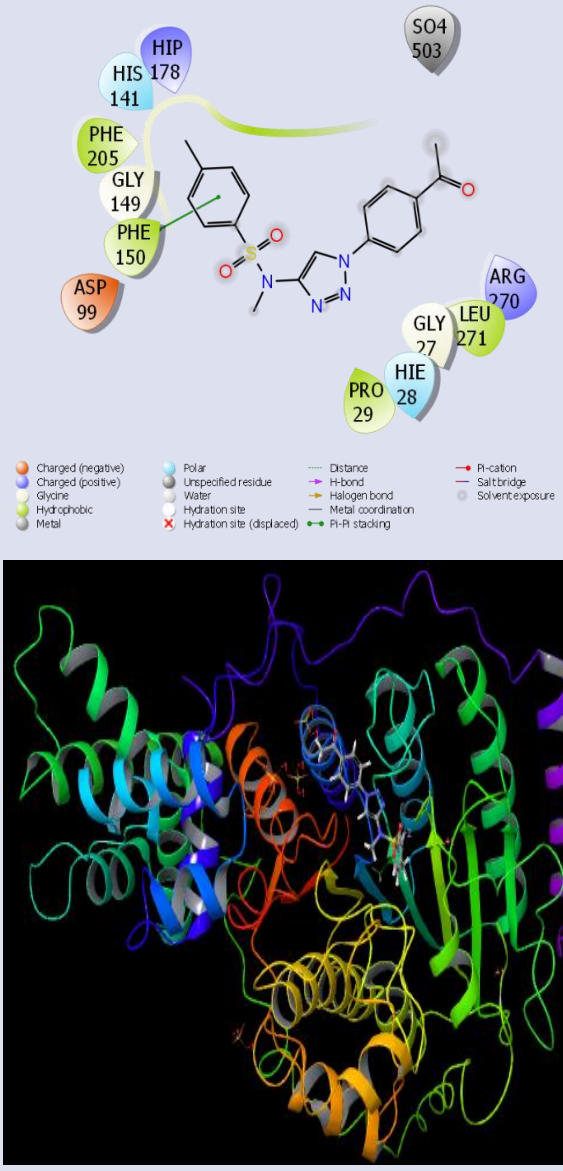

Figure 3. Presentation interactions of molecule 8 with 4BKX protein

The Glide ligand efficiency is the main parameter derived from molecular docking simulations. These are not the only complementary attributes. This numerical chart illustrates how well the ligand works against certain bacterial proteins. The Glide Hbond measures the quantity of hydrogen bonds formed during interactions between molecules and proteins [34]. The Van der Waals interaction number, often known as Glide Evdw [33], is another statistic that shows how chemicals and proteins interact. Additionally, a metric called Glide Ecoul is used to objectively evaluate the Coulomb interactions that occur between drugs and proteins. The Glide Einternal, a numerical value derived by integrating many components, is the last parameter derived from these computations [34].

Table 3. MM-GBSA parameter of molecule 4 with 4UYA protein

MMGBSA dG Bind	-31.79
MMGBSA dG Bind Coulomb	0.43
MMGBSA dG Bind Covalent	2.53
MMGBSA dG Bind Hbond	-0.95
MMGBSA dG Bind Lipo	-13.66
MMGBSA dG Bind Packing	-2.87
MMGBSA dG Bind Solv GB	0.00

MM-GBSA computations were used to ascertain the molecule's binding free energy values. The calculations revealed that the 4UYA protein and molecule 4 had the greatest negative docking score parameter. As a result, the energy values of molecule 4 against the 4UYA protein are shown in Table 3. According to the calculations, the binding free energy of molecule 4 among the 4UYA protein is -31.79. However, the obtained data showed that there were several interactions between the chemical and the protein. These interactions include the coulomb, covalent, Hbond, lipophilic, packing, SolvGB, and vdW interactions [35,36]. For example, the packing, lipophilic, and Hbond interactions seem to have a higher negative value.

Following an evaluation of the compounds' biological activity against various proteins, the ADME/T study was carried out to theoretically forecast the impacts and interactions of the most active molecules inside human metabolism [35]. Numerous factors were discovered throughout this theoretical investigation, as shown in Table 4.

ADME/T (Absorption, Distribution, Metabolism, Elimination/Toxicity) simulations utilizing Schrödinger Maestro software are crucial for evaluating the pharmacokinetic and toxicological properties of substances throughout the drug-development process. These simulations may be used to forecast how a potential chemical would behave in biological systems [36]. The Schrödinger program's QikProp module provides a comprehensive analysis of ADME/T parameters. Calculating and describing the following parameters is standard procedure. Molecular weight (MW) is a measure of a molecule's total atomic mass. A medication candidate is deemed successful according to Lipinski's "Rule of 5 [37]," if its molecular weight is fewer than 500 daltons. LogP (Hydrophobicity or Lipophilicity), which measures a molecule's lipophilicity, calculates the octanol/water partition coefficient. Potential toxicity or insufficient bioavailability may be indicated by both high and low LogP values. Generally speaking, a LogP number between 0 and 3 is optimal. Hydrogen Bond Donors and Acceptors (HBD/HBA) are the number of functional groups in a molecule that may create hydrogen bonds. The number of hydrogen bond donors (HBD) and hydrogen bond acceptors (HBA) affects a molecule's solubility and permeability across biological membranes.

Table 4. ADME properties of molecule

	1	2	3	4	5	6	7	8	Referance Range
mol_MW	358	342	370	363	346	373	400	370	130-725
dipole (D)	8.6	8.0	11.5	6.5	6.4	6.5	11.8	4.8	1.0-12.5
SASA	618	616	678	606	591	623	720	646	300-1000
FOSA	244	239	314	151	151	151	288	233	0-750
FISA	117	117	105	117	117	214	160	169	7-330
PISA	255	258	257	265	274	256	270	243	0-450
WPSA	2	2	2	73	49	2	2	2	0-175
volume (A^3)	1095	1080	1198	1064	1036	1094	1259	1141	500-2000
donorHB	0	0	0	0	0	0	0	0	0-6
accptHB	7.3	6.5	6.5	6.5	6.5	7.5	8.5	8.5	2.0-20.0
glob (Sphere =1)	0.8	0.8	0.8	0.8	0.8	0.8	0.8	0.8	0.75-0.95
QPpolrz (A^3)	37.5	37.6	41.7	37.0	36.0	37.5	43.6	39.3	13.0-70.0
QPlogPC16	11.0	10.9	11.9	11.3	10.3	11.7	13.0	11.7	4.0-18.0
QPlogPoct	17.1	16.7	18.6	16.6	16.1	17.3	20.6	18.0	8.0-35.0
QPlogPw	10.0	9.5	9.3	9.5	9.6	10.9	11.6	11.6	4.0-45.0
QPlogPo/w	2.4	2.7	3.5	2.9	2.6	1.6	2.6	1.7	-2.0-6.5
QPlogS	-3.6	-4.0	-5.0	-4.1	-3.7	-3.4	-4.6	-3.3	-6.5-0.5
CIQPlogS	-4.3	-4.3	-4.9	-4.8	-4.4	-4.5	-4.7	-4.0	-6.5-0.5
QPlogHERG	-5.5	-5.6	-5.9	-5.5	-5.5	-5.6	-6.3	-5.6	*
QPPCaco (nm/sec)	772	772	1004	770	766	92	301	248	**
QPlogBB	-0.8	-0.8	-0.8	-0.6	-0.6	-1.8	-1.5	-1.4	-3.0-1.2
QPPMDCK (nm/sec)	383	382	508	939	684	38	138	112	**
QPlogKp	-2.4	-2.5	-2.2	-2.5	-2.4	-4.2	-3.0	-3.4	Kp in cm/hr
IP (ev)	9.0	9.0	9.0	9.1	9.1	9.4	9.2	9.2	7.9-10.5
EA (eV)	0.9	1.0	1.0	1.2	1.2	2.1	1.5	1.5	-0.9-1.7
#metab	2	2	2	1	1	2	1	1	1-8
QPlogKhsa	-0.3	-0.1	0.2	-0.2	-0.2	-0.4	-0.2	-0.5	-1.5-1.5
Human Oral Absorption	3	3	3	3	3	3	3	3	-
Percent Human Oral Absorp.	93	94	100	95	94	71	86	80	***
PSA	77	68	69	69	69	114	105	98	7-200
RuleOfFive	0	0	0	0	0	0	0	0	Maximum is 4
RuleOfThree	0	0	0	0	0	0	0	0	Maximum is 3
Jm	0.5	0.1	0.0	0.1	0.2	0.0	0.0	0.1	-

* corcern below -5, **<25 is poor and >500 is great, *** <25% is poor and >80% is high.

In general, drug-like compounds should contain ten or less hydrogen bond acceptors (HBA) and five or fewer hydrogen bond donors (HBD) []. Total polar surface area, or TPSA, is the surface area of a molecule that is occupied by polar functional groups. TPSA is associated with the chemical's solubility and ability to cross biological membranes. Favorable bioavailability is indicated by a TPSA of less than 140 Å². Aqueous Solubility (LogS) is a metric used to quantify a molecule's solubility in water. The LogS value affects the formulation processes and the bioavailability of the medication candidate [34-36].

Bioavailability is typically restricted for compounds with low solubility. Plasma protein binding, or PPB, is the proportion of a substance that binds to plasma proteins. The drug's efficacy and free concentration may be lowered by increased binding to plasma proteins. Blood-brain barrier permeability is the ability of a substance to permeate the blood-brain barrier. Increased BBB permeability is beneficial for drugs used to treat central nervous system problems, whereas lower BBB permeability may reduce toxicity in systemic treatment. Metabolic Stability: Predicts the rate at which a drug will be broken down by liver enzymes. The drug's half-life is extended and its therapeutic effectiveness is enhanced by increased metabolic stability [35]. Hepatotoxicity and HERG Inhibition Toxicity Predictions: The possible cardiotoxicity of HERG channel inhibition is evaluated. The substance's potential for hepatotoxicity may be evaluated. The Caco-2 cell monolayer experiment replicates the translocation of a substance across the human intestinal epithelium. Increased Caco-2 permeability indicates better intestinal absorption. The absorption rate of a chemical predicts the proportion that will be absorbed when taken orally. A quick rate of absorption is an essential element of a successful pharmaceutical drug.

Lipinski's "Rule of Five" (RO5) is a guideline used to evaluate the pharmacological properties of a substance [38,39]. Determining the possibility that a chemical would have good oral bioavailability was the aim of these guidelines. The Rule of Five variables are Molecular Weight (MW), LogP, Hydrogen Bond Donors (HBD), and Hydrogen Bond Acceptors (HBA). The "Rule of Three" (RO3) is a criteria used in the pharmaceutical development process to identify lead molecules [40]. This rule, which is more stringent than RO5, focuses on the identification of low molecular weight, chemically simpler chemicals. For a molecule to be classified as a lead molecule under RO3, it must meet certain criteria. The Rule of Five includes the following criteria: Rotatable

Bonds, Hydrogen Bond Donors (HBD), Hydrogen Bond Acceptors (HBA), Molecular Weight (MW), and LogP. Since all parameters are expected to satisfy the criteria, the values of these two parameters are projected to be zero. Its calculations make it an essential tool for assessing toxicological risks at every stage of the drug development process. These simulations estimate the probability that a suggested chemical might negatively affect biological systems. Schrödinger, QikProp, and other modules are used to assess a range of toxicity parameters. The potassium ion channels known as HERG (Human Ether-à-go-go-Related Gene) channels regulate the electrical activity of cardiac myocytes. HERG Channel Inhibition (Cardiotoxicity) is the first parameter. Another criterion is blood-brain barrier (BBB) toxicity; drugs that can pass across the BBB may negatively impact the central nervous system [36]. Another measure is the substrate and inhibition of P-glycoprotein (P-gp). P-glycoprotein eliminates substances from cells, preventing dangerous accumulation.

Conclusions

In the present study, a comprehensive in silico approach was employed to investigate the electronic structure, chemical reactivity, and biological interaction potential of a series of benzenesulfonamide derivatives against key protein targets associated with gastric cancer. Utilizing density functional theory (DFT)-based Gaussian calculations, critical quantum chemical descriptors—such as frontier molecular orbital energies, chemical potential, and electrophilicity index—were determined, providing insights into the electronic distribution and stability of the molecules. These parameters not only elucidate the molecules' potential sites for nucleophilic and electrophilic attack but also support their thermodynamic favorability and chemical robustness in biological systems. Complementing the theoretical evaluations, molecular docking simulations were conducted to explore the binding affinities and interaction patterns of the studied compounds with two relevant gastric cancer-related proteins (PDB IDs: 4BKX and 3MAX). The docking results revealed that several benzenesulfonamide derivatives formed energetically favorable and geometrically stable complexes within the active sites of the target proteins, primarily via hydrogen bonding, hydrophobic contacts, and π–π stacking interactions. Notably, molecule 4 exhibited the most pronounced binding affinity toward the 4BKX protein with a docking score of −3.55, while molecule 8 demonstrated the highest affinity for the 3MAX protein, registering a docking score of −3.54. These results suggest that both molecules possess significant potential as lead structures for further optimization in gastric cancer drug discovery.

In addition to docking evaluations, ADME/T (Absorption, Distribution, Metabolism, Excretion, and Toxicity) predictions were performed using the QikProp module to assess the pharmacokinetic profiles and drug-likeness of the molecules. Although certain pharmacokinetic parameters—specifically QPPCaco and QPPMDCK, which are indicators of intestinal and cellular permeability—were observed to exceed ideal threshold values, potentially indicating suboptimal membrane penetration or blood–brain barrier permeability, the compounds demonstrated compliance with Lipinski's Rule of Five and the Rule of Three. These findings suggest that despite certain limitations in absorption-related parameters, the overall physicochemical characteristics and drug-likeness profiles of the compounds support their viability as orally administrable therapeutic candidates.

In conclusion, this integrated computational study underscores the potential of benzenesulfonamide derivatives as structurally and electronically suitable agents for targeting gastric cancer-related proteins. The favorable binding profiles, chemical stability, and compliance with drug-likeness rules collectively support their advancement into further stages of preclinical evaluation. Moreover, the findings contribute to a broader understanding of the structural features that govern ligand–target interactions in gastric cancer and offer a valuable platform for the rational design of novel, targeted chemotherapeutic agents.

Acknowledgments

The numerical calculations reported in this paper were fully/partially performed at TUBITAK ULAKBIM, High Performance and Grid Computing Center (TRUBA resources). This work was supported by the Scientific Research Project Fund of Sivas Cumhuriyet University (CUBAP) under the project number RGD-020.

Conflicts of Interest

The author declare no competing financial interest or personal relationships.

References

[1] Acar Cevik U., Ünver H., Bostancı H. E., Tüzün B., Gedik N. İ., Kocyigit Ü. M., New hydrazone derivatives: synthesis, characterization, carbonic anhydrase I-II enzyme inhibition, anticancer activity and in silico studies. Zeitschrift für Naturforschung C., (2025) (0) article in press.

[2] Allah A. E. M. A., Mortada S., Tüzün B., Guerrab W., Qostal M., Mague J. T., Ramli Y., Novel Thiohydantoin Derivatives: Design, Synthesis, Spectroscopic Characterization, Crystal Structure, SAR, DFT, Molecular Docking, Pharmacological and Toxicological activities, *Journal of Molecular Structure,* (2025) 141995.

[3] Karatas H., Kul İ. B., Aydin M., Tüzün B., Taslimi P., Kokbudak Z., Alzheimer's Disease Drug Design by Synthesis, Characterization, Enzyme Inhibition, In Silico, SAR Analysis and MM-GBSA Analysis of Schiff Bases Derivatives, *Korean Journal of Chemical Engineering*, (2025) 1-19.

[4] Şahin İ., Çeşme M., Güngör Ö., Özgeriş F. B., Köse M., Tümer, New sulfonamide derivatives based on 1, 2, 3-triazoles: synthesis, in vitro biological activities and in silico

studies, *Journal of Biomolecular Structure and Dynamics*, 42(9) (2024) 4782-4799.

[5] Becke A.D., Density-functional thermochemistry. I. The effect of the exchange-only gradient correction, *The Journal of Chemical Physics*, 96(3) (1992) 2155-2160.

[6] Vautherin D., Brink D. T., Hartree-Fock calculations with Skyrme's interaction. I. Spherical nuclei, *Physical Review C*, 5(3) (1972) 626.

[7] Hohenstein E. G., Chill S. T., Sherrill C. D., Assessment of the performance of the M05− 2X and M06− 2X exchange-correlation functionals for noncovalent interactions in biomolecules, *Journal of Chemical Theory and Computation*, 4(12) (2008) 1996-2000.

[8] Bressi, J. C., Jennings, A. J., Skene, R., Wu, Y., Melkus, R., De Jong, R., ... & Gangloff, A. R. Exploration of the HDAC2 foot pocket: Synthesis and SAR of substituted N-(2-aminophenyl) benzamides, *Bioorganic & Medicinal Chemistry Letters,* 20(10) (2010) 3142-3145.

[9] Millard C. J., Watson P. J., Celardo I., Gordiyenko Y., Cowley S. M., Robinson C. V., Schwabe J. W., Class I HDACs share a common mechanism of regulation by inositol phosphates, *Molecular Cell*, 51(1) (2013) 57-67.

[10] Dennington R., Keith T. A., Millam J. M., GaussView 6.0. 16. Semichem Inc.: Shawnee Mission, KS, (2016) USA.

[11] Frisch M.J., Trucks G.W., Schlegel H.B., Scuseria G.E., Robb M.A., Cheeseman J.R., Scalmani G., Barone V., Mennucci B., Petersson G.A., Nakatsuji H., Caricato M., Li X., Hratchian H.P., Izmaylov A.F., Bloino J., Zheng G., Sonnenberg J.L., Hada M., Ehara M., Toyota K., Fukuda R., Hasegawa J., Ishida M., Nakajima T., Honda Y., Kitao O., Nakai H., Vreven T., Montgomery J.A., Peralta J.E., Ogliaro F., Bearpark M., Heyd J.J., Brothers E., Kudin K.N., Staroverov V.N., Kobayashi R., Normand J., Raghavachari K., Rendell A., Burant J.C., Iyengar S.S., Tomasi J., Cossi M., Rega N., Millam J.M., Klene M., Knox J.E., Cross J.B., Bakken V., Adamo C., Jaramillo J., Gomperts R., Stratmann R.E., Yazyev O., Austin A.J., Cammi R., Pomelli C., Ochterski J.W., Martin R.L., Morokuma K., Zakrzewski V.G., Voth G.A., Salvador P., Dannenberg J.J., Dapprich S., Daniels A.D., Farkas O., Foresman J.B., Ortiz J.V., Cioslowski J.,Fox D.J. (2009) Gaussian 09, revision D.01. Gaussian Inc, Wallingford CT

[12] Medetalibeyoğlu H., Atalay A., Sağlamtaş R., Manap S., Ortaakarsu A. B., Ekinci E., Tüzün B., Synthesis, design, and cholinesterase inhibitory activity of novel 1, 2, 4-triazole Schiff bases: A combined experimental and computational approach, *International Journal of Biological Macromolecules*, 306 (2025) 141350.

[13] Akkus M., Kirici M., Poustforoosh A., Erdogan M. K., Gundogdu R., Tüzün B., Taslimi P., Phenolic Compounds: Investigating Their Anti-Carbonic Anhydrase, Anti-Cholinesterase, Anticancer, Anticholinergic, and Antiepileptic Properties Through Molecular Docking, MM-GBSA, and Dynamics Analyses, *Korean Journal of Chemical Engineering*, (2025) 1-20.

[14] Schrödinger Release 2022-4: Maestro, Schrödinger, LLC, New York, NY, 2022.

[15] Schrödinger Release 2022-4: Protein Preparation Wizard; Epik, Schrödinger, LLC, New York, NY, 2022; Impact, Schrödinger, LLC, New York, NY; Prime, Schrödinger, LLC, New York, NY, 2022

[16] Schrödinger Release 2022-4: LigPrep, Schrödinger, LLC, New York, NY, 2022.

[17] Shahzadi I., Zahoor A. F., Tüzün B., Mansha A., Anjum M. N., Rasul A., Mojzych M., Repositioning of acefylline as anti-cancer drug: Synthesis, anticancer and computational studies of azomethines derived from acefylline tethered 4-amino-3-mercapto-1, 2, 4-triazole, *Plos One*, 17(12) (2022) e0278027.

[18] El Faydy M., Lakhrissi L., Dahaieh N., Ounine K., Tüzün B., Chahboun N., Zarrouk A. Synthesis, Biological Properties, and Molecular Docking Study of Novel 1, 2, 3-Triazole-8-quinolinol Hybrids, *ACS omega*, 9(23) (2024) 25395–25409.

[19] Schrödinger Release 2022-4: QikProp, Schrödinger, LLC, New York, NY, 2022.

[20] Ullah N., Alam A., Tüzün B., Rehman N. U., Ayaz M., Elhenawy A. A., Ahmad M., Synthesis of novel thiazole derivatives containing 3-methylthiophene carbaldehyde as potent anti α-glucosidase agents: In vitro evaluation, molecular docking, dynamics, MM-GBSA, and DFT studies. *Journal of Molecular Structure*, 1321 (2025) 140070.

[21] Yalazan H., Koç D., Aydın Kose F., Fandaklı S., Tüzün B., Akgül, M. İ, Kantekin H. Design, syntheses, theoretical calculations, MM-GBSA, potential anti-cancer and enzyme activities of novel Schiff base compounds, *Journal of Biomolecular Structure and Dynamics,* 42(23) (2024) 13100-13113.

[22] Manap S., Medetalibeyoğlu H., Kılıç A., Karataş O. F., Tüzün B., Alkan M., Yüksek H., Synthesis, molecular modeling investigation, molecular dynamic and ADME prediction of some novel Mannich bases derived from 1, 2, 4-triazole, and assessment of their anticancer activity, *Journal of Biomolecular Structure and Dynamics*, 42(21) (2024) 11916-11930.

[23] Rafik A., Tuzun B., Zouihri H., Poustforoosh A., Hsissou R., Elhenaey A. A., Guedira T., Morphology studies, optic proprieties, hirschfeld electrostatic potential mapping, docking molecular anti-inflammatory, and dynamic molecular approaches of hybrid phosphate, *Journal of the Indian Chemical Society*, 101(11) (2024) 101419.

[24] Barghady N., Assou S. A., Er-Rajy M., Boujdi K., Arzine A., Rhazi Y., El Yazidi M., Design, synthesis, characterization, and theoretical calculations, along with in silico and in vitro antimicrobial proprieties of new isoxazole-amide conjugates, *Open Chemistry*, 22(1) (2024) 20240109.

[25] Schrader T., Khanifaev J., Perlt E., Koopmans' theorem for acidic protons, *Chemical Communications*, 59(93) (2023) 13839-13842.

[26] Phillips J. C., Generalized Koopmans' Theorem., *Physical Review*, 123(2) (1961) 420.

[27] Pearson R. G., Hard and soft acids and bases, *Journal of the American Chemical Society*, 85(22) (1963) 3533-3539.

[28] Pearson R. G., Hard and soft acids and bases, *Journal Of The American Chemical Society*, 85(22) (1963) 3533-3539.

[29] Ayers P. W., An elementary derivation of the hard/soft-acid/base principle, *The Journal of Chemical Physics*, 122(14) (2005).

[30] Parr R. G., Chattaraj P. K., Principle of Maximum Hardness, *Journal of the American Chemical Society*, 113(5) (1991) 1854-1855.

[31] Goswami A. K., Aboul-Soud M. A., Gogoi N., El-Shazly M., Giesy J. P., Tüzün B., Sharma H. K., Integrative in silico evaluation of the antiviral potential of terpenoids and its metal complexes derived from Homalomena aromatica based on main protease of SARS-CoV-2, *Open Chemistry,* 22(1) (2024) 20240085.

[32] Medetalibeyoğlu H., Manap S., Alkan M., Beytur M., Barlak N., Karatas O. F., Taslimi P., Novel Schiff Bases: Synthesis, characterization, bioactivity, cytotoxicity, and computational evaluations, *Polycyclic Aromatic Compounds*, (2024) 1-19.

[33] Tapera M., Kekeçmuhammed H., Tüzün B., Daştan S. D., Çelik M. S., Taslimi P., Sarıpınar E., Novel 1, 2, 4-triazole-maleamic acid derivatives: Synthesis and evaluation as anticancer agents with carbonic anhydrase inhibitory activity, *Journal of Molecular Structure*, 1313 (2024) 138680.

[34] Alishba Ali I., Hameed S., Khan K. M., Salar U., Taha M., Ulukaya E., Exploring Benzo [b][1, 4] Thiazine Derivatives: Multitarget Inhibition, Structure–Activity Relationship, Molecular Docking, and ADMET Analysis, *ChemistrySelect*, 9(38) (2024) e202404087.

[35] Belkheiri A., Dahmani K., Mzioud K., Rbaa M., Galai M., Hmada A., Al-Maswar, B. M., Advanced evaluation of novel quinoline derivatives for corrosion inhibition of mild steel in acidic environments: A comprehensive electrochemical, computational, and surface study, *International Journal of Electrochemical Science*, 19(10) (2024) 100772.

[36] Çelik M. S., Kütük N., Yenidünya A. F., Çetinkaya S., Tüzün B., Removal of safranin O from wastewater using Streptomyces griseobrunneus dead biomass and in silico calculations, *Biomass Conversion and Biorefinery*, 14(20) (2024) 25873-25884.

[37] Zahirović A., Fočak M., Fetahović S., Tüzün B., Višnjevac A., Muzika V., Roca S., Hydrazone-flavonol based oxidovanadium (V) complexes: Synthesis, characterization and antihyperglycemic activity of chloro derivative in vivo, *Journal of Inorganic Biochemistry*, 258 (2024) 112637.

[38] Lipinski C. A., Lead-and drug-like compounds: the rule-of-five revolution, *Drug Discovery Today: Technologies,* 1(4) (2004) 337-341.

[39] Lipinski C. A., Lombardo F., Dominy B. W., Feeney P. J., Experimental and computational approaches to estimate solubility and permeability in drug discovery and development settings, *Advanced Drug Delivery Reviews*, 23 (1997) 3-25.

[40] Jorgensen W.J., Duffy E.M., Prediction of drug solubility from structure, Advanced Drug Delivery Reviews, 54(3) (2002) 355-366.